Cyclin-Dependent Kinase Inhibition by New C-2 Alkynylated Purine Derivatives and Molecular Structure of a CDK2−Inhibitor Complex

Michel Legraverend,*,§ Paul Tunnah,‡ Martin Noble,‡ Pierre Ducrot,§ Odile Ludwig,§ David S. Grierson,§ Maryse Leost,† Laurent Meijer,† and Jane Endicott*,‡

Section de Recherche, Institut Curie, UMR 176 CNRS, Bât. 110-112, Centre Universitaire, 91405 Orsay Cedex, France, Station Biologique, CNRS, B.P. 74, 29682 Roscoff Cedex, France, and Department of Biochemistry, Laboratory of Molecular Biophysics and Oxford Centre for Molecular Sciences, Rex Richards Building, South Parks Road, Oxford OX1 3QU, U.K.

Received June 30, 1999

A new series of 2,6,9-trisubstituted purines, characterized by the presence of a common alkynyl substituent at C-2 and a range of different anilino/benzylamino groups at C-6, were synthesized. These compounds were evaluated for their capacity to inhibit cyclin-dependent kinase activity (CDK1−cyclin B) in vitro. Compounds **4e** (*N*-6-*p*-Cl-benzylamino derivative) and **5e** (*N*-6-*m*-Cl-anilino derivative) exhibited the strongest inhibitory activity with an IC_{50} of 60 nM. The structure of compound **4b** (*N*-6-*p*-methoxybenzylamino derivative) in complex with human CDK2 was determined by X-ray crystallography, revealing the molecular basis of inhibition by this molecule. Subsequent molecular modeling studies allowed us to rationalize the SAR observed for these compounds.

Introduction

Cyclin-dependent kinases (CDKs), particularly CDK1, CDK2, CDK4, and CDK6, play important roles in cell cycle regulation. Their sequential activation ensures the correct timing and ordering of events required for cell cycle progression.[1] Over the past decade, intense efforts, using biochemical and molecular biology techniques, have helped to define the mechanism of action of the CDKs, their regulation, and the identity of certain of their protein substrates.[2] To advance such studies, small molecule cyclin-dependent kinase inhibitors (CKIs) would be valuable biochemical tools.

Similarly, taking into consideration that CDK misregulation is implied in a number of disease states, and in particular cancer, enormous potential exists for small molecule CKIs as chemotherapeutic agents.[3] Indeed, certain proteins that regulate CDKs (e.g. the CKI p16 and cyclin D) or are CDK substrates (e.g. the retinoblastoma protein, pRb) are incorrectly or inappropriately expressed in a number of proliferative disorders. Both pRb and certain CKIs have been characterized as tumor suppressors.[4,5]

The development of selective inhibitors for the ATP binding site is, to a large extent, rendered difficult by the high level of sequence homology that exists for this region among protein kinases.[6,7] However, the screening of compound collections has revealed that small molecules are indeed able to selectively inhibit the CDK family. For example, the 2,6,9-trisubstituted purines olomoucine and roscovitine selectively inhibit CDK1−cyclin B, CDK2−cyclin E/A, and CDK5−p35.[8,9]

Building upon this discovery, more optimized purine CKIs have been described by several groups. These include the potent purine derivatives bearing a diaminocyclohexane substituent at C-2, described by the Novartis group,[10] and purvalanols A and B, identified by Schultz et al. by combinatorial library evaluation.[11,12] Flavopiridol,[13] indirubin 3′-monoxime[14] (the active ingredient in a traditional Chinese herbal medicine historically used to treat chronic myelocytic leukemia), and kenpaullone[15] represent different families of molecules (Figure 1) which also interact with the ATP binding site in CDK1/CDK2.

In our laboratory, a new series of potent and selective trisubstituted purine-based CKIs is being developed.[16] These systems are characterized by the presence of a hydroxyalkyl-substituted acetylene substituent at C-2 of the purine ring. For example, compound **4a** is a more potent inhibitor of CDK1−cyclin B (IC_{50} = 200 nM) than the lead molecule (*R,S*)-roscovitine (IC_{50} = 650 nM).

Although no structures have been obtained to date for CDK1, X-ray crystal structures of CDK2 complexes with ATP,[17] olomoucine,[18] roscovitine,[19] staurosporine,[20] flavopiridol,[13] purvalanol B,[11] and indirubin[14] have been reported which demonstrate how the ATP binding site can accommodate structurally diverse inhibitor types. X-ray structures for CDK2−cyclin A−ATP,[21] CDK2 alone,[17] and CDK2−cyclin A plus $p27^{KIP122}$ (natural CKI) have also been determined. These structures have shown how movements of the T-loop, PSTAIRE region, and N- and C-terminal lobes induced by cyclin binding and CDK2 Thr160 phosphorylation result in a catalytically active complex.[21] They also reveal limited differences in the vicinity of the ATP adenine binding site between different activation states of CDK2. This suggests that information derived from monomeric CDK2−inhibitor structures can guide the design of inhibitors against the active binary complex.

In this context, this report presents further advances in the development of the novel C-2 alkynyl-substituted purine family of CKIs. A series of molecules bearing a range of different anilino/benzylamino groups at C-6 has

* To whom correspondence should be addressed. M. Legraverend: tel, 1-6986-3086; e-mail, Michel.Legraverend@curie.u-psud.fr.
§ UMR 176 CNRS.
† CNRS.
‡ Laboratory of Molecular Biophysics and Oxford Centre for Molecular Sciences.

10.1021/jm9911130 CCC: $19.00
Published on Web 03/11/2000

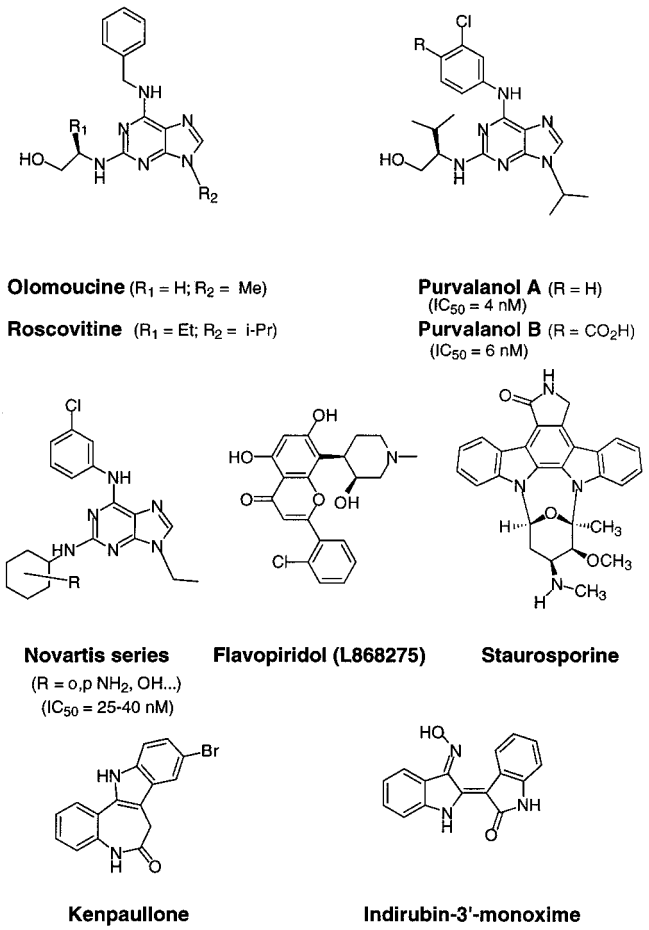

Figure 1. Structures of CKIs.

thus been synthesized and evaluated for their capacity to inhibit CDK1−cyclin B in vitro. All compounds prepared proved to be more active than roscovitine, with maximum activity observed for **4e** and **5e** (IC_{50} = 60 nM). The structure of one of these compounds, OL567 (**4b**) in complex with CDK2, was determined by X-ray crystallography, revealing the molecular basis of inhibition by this molecule. Subsequent molecular modeling, employing the crystal structure data, has further permitted us to rationalize the structure−activity relationship (SAR) observed for these compounds.

Chemistry

To access the C-2 alkynylated purine compounds **4b**−**h** and **5a**−**e**, 6-chloro-2-iodo-9-isopropyl-(9*H*)-purine **(1)**, prepared as previously described,[16,23−25] was reacted with the appropriate meta- and/or para-substituted anilines or benzylamines (1.5 equiv) in ethanol containing $N(Et)_3$ (4 equiv), under inert atmosphere at 50 °C for 3−4 h (Scheme 1). In this way the C-6 substituted purine derivatives **2** and **3** were obtained in high yields (60−95%). Conversion of these 2-iodopurine intermediates to the target 2-ethynylpurines **4** and **5** was achieved by reaction with 3-methylpent-1-yn-3-ol under palladium(0)-CuI catalyzed cross-coupling conditions developed by Sonogashira.[26]

Table 1. IC_{50} Values against CDK1−Cyclin B for Members of Series **4** and **5**

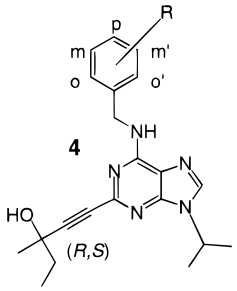

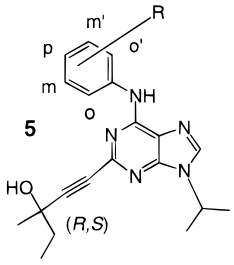

compd[a]	R	IC_{50} (nM)
4a	H	200
4b (OL567)	*p*-OCH_3	230
4c	*p*-OCH_2CH_3	180
4d	*m*,*p*-di-Cl	430
4e	*p*-Cl	60
4f	*m*,*p*-OCH_2O	200
4g	*m*,*p*-di-OCH_3	300
4h	*p*-$N(CH_3)_2$	150
5a	H	400
5b	*p*-OCH_3	200
5c	*p*-OCH_2CH_3	200
5d	*m*,*p*-di-Cl	200
5e	*m*-Cl	60
olomoucine		7000
(*R*,*S*)-roscovitine		650

[a] *m* = meta, *p* = para substituents of the phenyl group.

Results and Discussion

Compounds **4** and **5** were tested for their ability to inhibit in vitro the CDK1−cyclin B complex from starfish oocytes as described.[9,16,25] In this assay the transfer of γ-^{32}P-labeled phosphate from ATP to histone H1 in the absence and presence of inhibitor is measured and expressed as a percent of kinase activity without inhibitor. The IC_{50} is determined from dose−response curves. The IC_{50} value for each of the compounds determined under these assay conditions is shown in Table 1.

Trisubstituted purine-based inhibitors of CDK1−cyclin B, and in particular those bearing an amino

Scheme 1[a]

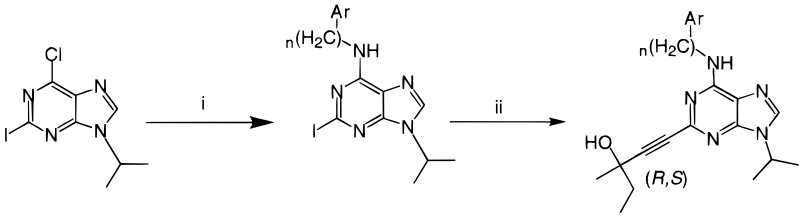

[a] (i) Aniline or benzylamine (1.5 equiv), $N(Et)_3$ (4 equiv), ethanol, 50 °C, 3−4 h; (ii) (*R*,*S*)-3-methyl-1-pentyn-3-ol (1.5 equiv), CuI (0.05 equiv), dichlorobis(triphenylphosphine)palladium(II) (0.01 equiv), *n*-butylamine (1.5 equiv), degassed DMF (25 mL), 80 °C.

alcohol substituent at C-2, generally, also inhibit CDK2 and CDK5 to various extents.[8,9,11] For this reason compounds **4** and **5** were evaluated for their capacity to inhibit CDK5−p25 (data not shown). With the exception of compound **4f**, which is more active in the CDK5 assay (IC_{50} = 130 nM), all compounds in both series displayed reduced capacity to inhibit CDK5−p25. This is especially true for the monochloro analogues **4e** and **5e**, which are respectively 4 and 8.3 times less active against CDK5−p25. These results are not included in our SAR study as X-ray crystal data for CDK5 is currently unavailable. Note, however, that two recent publications describe computer-generated models of CDK5 either alone[27] or complexed to a neuronal CDK5 activator (Nck5a).[28]

Taking roscovitine as reference (IC_{50} = 650 nM) it was found that the purine derivative **4a**, which is unsubstituted in the phenyl ring of the 6-benzylamine group, is 3 times more active.[16] Indeed, all the new C-2 alkynylated purine compounds **4** containing a meta and/or para substituent on the phenyl ring are more active than roscovitine. These results underscore our preliminary finding that there is a gain in activity upon exchange of the 2-amino alcohol chain in roscovitine by a propargyl alcohol motif.[16]

In the present study, the first modification of **4a** to be examined was the introduction of a *p*-OMe substituent.[29,30] Interestingly, a slight loss in activity was observed for the derived compound **4b** (OL567). Introduction of a second OMe group to give the *m*,*p*-dimethoxyphenyl analogue **4g** resulted in a further loss in activity, whereas the methylenedioxy analogue **4f** remained equipotent with **4a**. These results contrast with the small gain in activity for the corresponding *p*-OEt-substituted compound **4c**.

The largest fluctuation in activity was observed for the chloro-substituted analogues **4d** and **4e**. Compound **4d** with chlorine atoms at both the meta and para positions of the phenyl ring proved to be the least active molecule in the series, whereas compound **4e** with a single *p*-chloro substituent displayed powerful capacity to inhibit substrate phosphorylation by CDK1−cyclin B (IC_{50} = 60 nM). This latter finding suggested that the presence of a polar substituent at the para position of the phenyl ring of the 6-benzylamino should be favorable. The good level of activity observed for the *p*-NMe_2-substituted analogue **4h** is consistent with this idea.

The preparation of compounds **5a**−**e** was undertaken on the basis of independent reports by the Novartis group, Schultz et al., and ourselves[10,11,25,31] which showed that trisubstituted purines possessing a substituted arylamine at C-6 were active. It was interesting to find therefore that, relative to the parent anilino compound **5a**, good levels of activity were observed for compounds **5b**−**e** bearing meta−para substituents and that analogue **5e** with a *m*-chloro group is equipotent with **4e**.

To summarize the data, the best results were obtained with *m*- or *p*-chloro substituents on the aminophenyl (anilino) and benzylamino groups, respectively. These results confirm that the capacity of the C-2 alkynyl-substituted purines to inhibit CDK1−cyclin B can be modulated through variation of the C-6 position aromatic ring substituents. This point is of considerable importance as the specificity and potency of olomoucine, roscovitine, and OL567 are in part the consequence of interaction of their 6-aminobenzyl substituent with a region of the kinase that is highly conserved in the CDK family and which does not interact with its natural substrate, ATP.[19,32] To obtain more information on this point the structure of the CDK2−**4b** (OL567) complex was determined by X-ray diffraction.

Crystallographic Analysis: Interactions between CDK2 and OL567. The structure of CDK2 is a minimal protein kinase catalytic core consisting of an N-terminal domain formed principally from β-sheet and a C-terminal domain that is primarily α-helical.[17,33] OL567 occupies the binding site in the cleft between the CDK2 N- and C-terminal domains. Figure 2 shows the hydrogen-bonding pattern and apolar contacts of OL567 bound to CDK2 as calculated by the program Ligplot.[34] The apolar contacts correspond to contacts shorter than 3.9 Å between non-hydrogen-bonding atom pairs.

The binding of OL567 to CDK2 closely resembles that of olomoucine,[18] roscovitine,[19] and purvalanol[11] and differs from that reported for ATP bound to CDK2.[17] OL567 N7 accepts a hydrogen bond from the peptide nitrogen of Leu83, and N6 of OL567 donates a hydrogen bond to the backbone oxygen of Leu83. The ATP adenine ring hydrogen bonds to the CDK2 backbone in this region through interactions between N6 and the backbone oxygen of Glu81 and between N1 and the backbone nitrogen of Leu83. The OL567 adenine ring is sandwiched between the side chains of Ile10 and Leu134 and is not coplanar with that of the ATP adenine ring in the CDK2−ATP structure. Minor variations in ring position between OL567, olomoucine, roscovitine, and purvalanol are observed.[11,13,35,36]

Although residues 80−84 constitute part of the hinge between the CDK2 N- and C-terminal domains, the interactions do not result in a significant change in relative domain orientation.

OL567, like roscovitine, has an isopropyl group on N9 that forms hydrophobic contacts with the side chain of Phe80. As commented upon in more detail further on, the 3-methylpent-1-yn-3-ol group substituted at C-2 binds in the pocket occupied by the ATP ribose group in the phosphorylated CDK2−cyclin A binary complex.[37] Binding appears to favor the *S* isomer which places the methyl group into a small hydrophobic patch formed mainly by Val18 and backbone atoms of the glycine loop at residues 11 and 12. However, interpretation of the electron density map for this group is not unambiguous. Val18 shows slight movement toward the inhibitor to maximize the hydrophobic contact. Bound as the *S* isomer, the hydroxyl group makes no direct interactions with CDK2 but can hydrogen bond to a bound water molecule (Figure 2).

The 4-methoxybenzylamino group on N6 is surface exposed and binds outside the active side cleft contacting residues in the hinge region and N-terminal lobe (Figure 2). The phenyl ring is surrounded by the side chains of Phe82 and Ile10, the side chain amino group of Lys89, and the CDK2 backbone at His84. Olomoucine, roscovitine, purvalanol B, and OL567 all have markedly different ring orientations, that of OL567 being most displaced from that of purvalanol B. Lys89 adopts a different conformation to that seen in the olomoucine

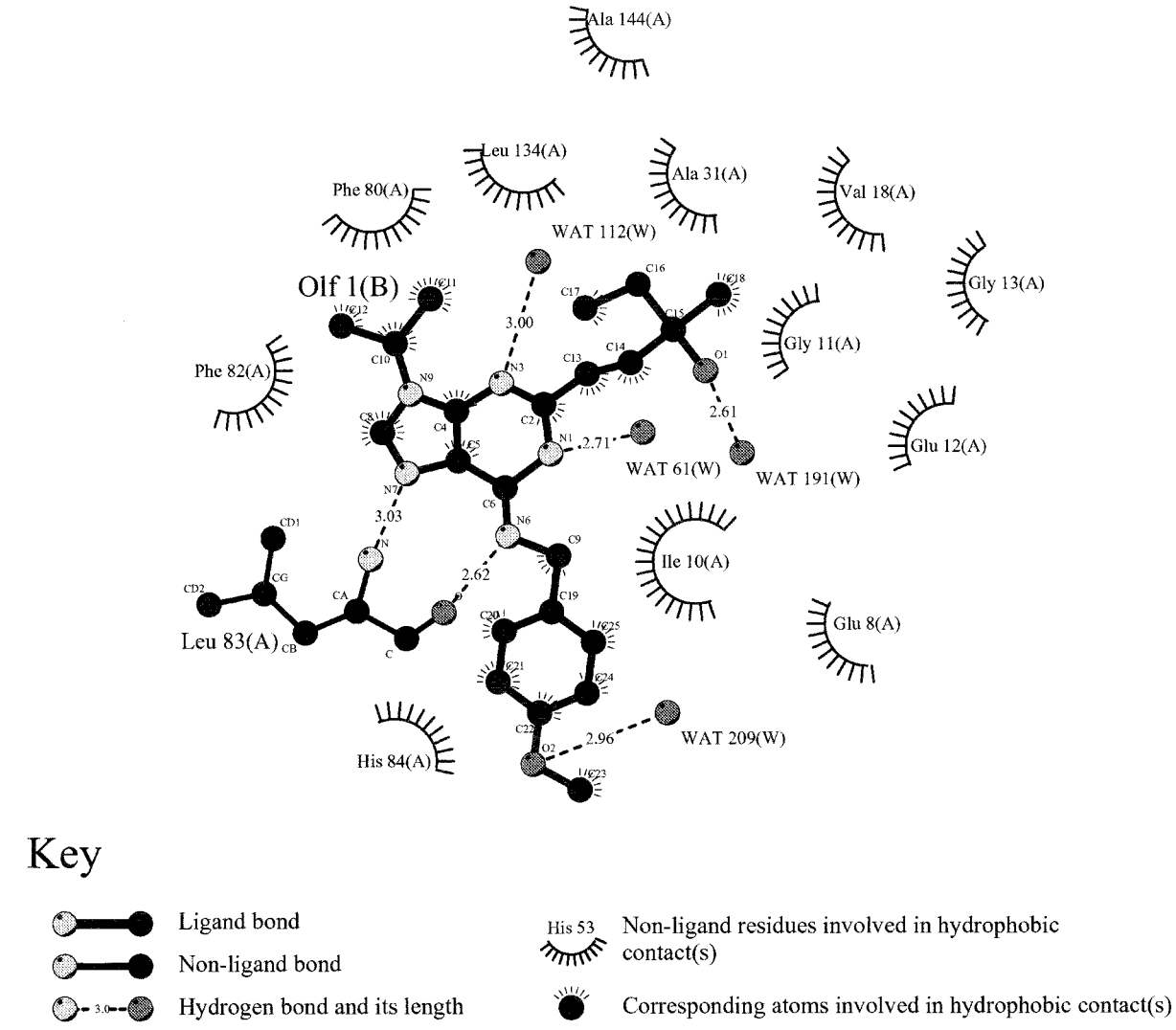

Figure 2. Schematic representation of the contacts between OL567 and CDK2 produced using Ligplot. Hydrogen-bonding residues are drawn in full, with the length of the hydrogen bond annotated on a dotted line. Residues making non-hydrogen-bonding contacts at a distance of less than 3.9 Å are also drawn, with a 'fan' representation indicating the atom of CDK2 contacted.

structure,[18] being oriented toward Asp86. To avoid a steric clash, the 4-methoxy group displaces the side chain of Glu8. The combination of this movement and also that of Val 18 results in subtle differences in the positions of the residues throughout the glycine-rich loop.

Molecular Modeling. OL567 is intermediate in its capacity to inhibit CDK1−cyclin B relative to the monochloro compound **4e** and compound **4d** which possesses a *m*,*p*-dichlorobenzylamino substituent at C-6. Several factors could be acting individually or collectively to give rise to this range of activities, including steric interactions due to the presence of functionality on the phenyl ring and electronic effects. Steric interactions can lead to a local repositioning of the benzyl side chain in its binding zone (rotation about C−C/C−N bond) or to a repositioning of the entire molecule in the ATP binding pocket. To better understand the influence of the C-6 substituent on inhibition within this series of purine derivatives, and to study the binding of the corresponding anilino compounds **5** in the ATP pocket of CDK1, molecular models were developed using the crystal data for the OL567−CDK2 complex as the starting point. This approach was considered valid in view of the very high degree of sequence homology between CDK1 and CDK2 for the amino acid residues that comprise the ATP binding pocket (Table 2). Indeed, two important residues are modified in the catalytic site of the two kinases (CDK2: His84, Gln85 → Ser84, Met85: CDK1), which both have their respective side chains outside the binding pocket and are not directly involved in ATP binding.

Compounds **4b**−**h** and **5a**−**e** were constructed in Sybyl 6.5.1 (Tripos software) using the structure for OL567 (**4b**) extracted from the crystallographic data. Conformations were generated for the phenyl moiety by systematic rotations (60° step) around all bonds attached to the aromatic ring; then each conformer was docked separately. For the protein, all hydrogens and lone pairs were added, and Kollman charges were included such that the amine and carboxylic acid functions were all ionized (NH_3^+, CO_2^-; pH 7). In addition, hydrogens were added to the ligand, and Gasteiger−Hückel charges were calculated within SYBYL. Docking calculations, were then carried out after residues within 15 Å from the ligand (OL567) were extracted. The molecules were docked using the DOCK module within Sybyl, maintaining the binding site rigid

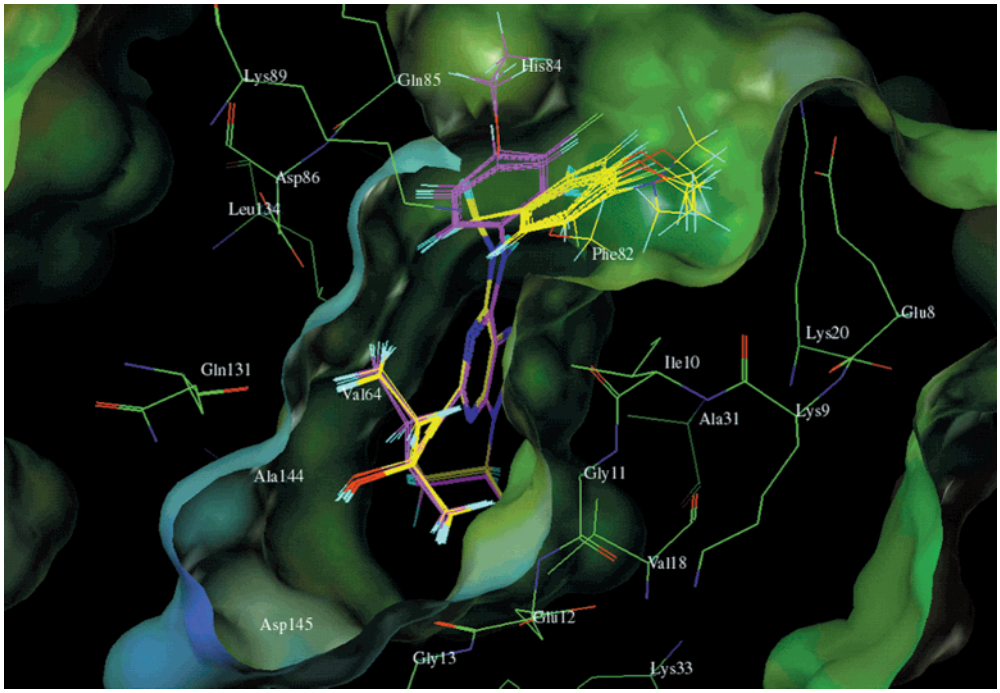

Figure 3. Superimposition of *N6*-benzylaminopurine series **4b**−**h** (yellow) and *N6*-phenylaminopurine series **5b**−**e** (magenta) as modeled in the ATP binding site of human CDK2. The enzyme is colored using a lipophilicity range from brown (highest lipophilic area of the molecule) to blue (highest hydrophilic area); intermediate lipophilicity is in green.

during minimizations. After minimization was completed, the best conformer hits for each compound were reminimized within the binding site without any rigid body. Figure 3 shows the superimposition of the minimum energy structures for the two series docked in the ATP binding site.

In Figure 3, one sees that, relative to OL567 (**4b**), there is essentially no change in the position of the purine ring and the C-2 acetylene side chain in compounds **4c**−**h**. A complete superposition of these elements in compounds **5** was also observed, indicating that modification of the C-6 substituent does not provoke any significant displacement of the molecule in the ATP site. This is consistent with the relatively small variations in activity that are observed.

As might be expected, the aromatic rings of the C-6 benzylamino and anilino groups in analogues **4** and **5** occupy different regions of space in the enzyme. Consequently, there is a distinct set of interactions for the functionalized aryl rings in each series with the amino acid residues in their vicinity.

In Figure 4 a more focused view of the positioning and environment of the aromatic ring of the *N*-benzyl compounds **4b**−**h** in the ATP pocket is given. In particular, one sees that the pocket is composed of two hydrophobic residues (Ile10, Phe82), which interact and limit the movement of the aromatic ring, as well as three important polar residues (His84, Lys20, Glu8).

Considering the different analogues individually, it is striking that the *m*,*p*-dichloro analogue **4d**, which displays the weakest activity, is oriented in a manner opposite to the two other more bulky meta,para-disubstituted analogues **4f** and **4g**. Indeed, comparison of the relative energies of the meta/para orientation of **4d** with its alternative meta′/para conformer indicates that the latter is 3 kcal/mol less stable. This energy difference results from the fact that, even though the "meta" side of the aromatic ring is globally more crowded by the presence of Phe82, a larger volume is available in the immediate vicinity of the meta carbon.

As this advantage is lost for compounds **4f** and **4g** with more bulky and extended alkoxy substituents, they prefer to adopt the meta′/para conformation ($\Delta E = 6.42$ kcal). Oriented in this way, the oxygen substituents experience the more hydrophilic environment created by residues Lys89 and Glu8 and the backbone amide carbonyl oxygens of Ile10 and Lys9 located toward the exterior of the kinase. Steric crowding remains, however, a problem in this orientation. This is particularly true for compound **4g**, in which the *m*′-OMe group points toward the para substituent, rather than away from it, in an effort to avoid Lys89 and the acetylenic side chain. In the methylenedioxy analogue **4f** this steric interaction is diminished.

Although no ortho-substituted compounds were evaluated in this study, the model predicts that there is no place to accommodate functionality in the ortho conformation due to the presence of the Phe82 residue. Equally severe problems would be encountered for the ortho′ conformer due to unfavorable interactions with both Lys89 (at 2 Å) and the purine ring of the inhibitor itself (3.4 Å from the ethyl chain of the *R* isomer, 4.8 Å from the OH of the *S* isomer, and 4.5 Å from the triple bond).

In contrast to the dichloro analogue **4d**, compound **4e** with one *p*-chloro substituent proved to be the most active inhibitor of CDK1−cyclin B. From comparison of this analogue with the parent unsubstituted compound **4a** and the olomoucine−CDK2 structure, it may be expected that the presence of the electron-withdrawing chloro substituent in **4e** might be detrimental to a CH−π type interaction[38] with the side chain of Ile10. However, it is difficult to appreciate the influence of the chloro substituent on this already inherently weak

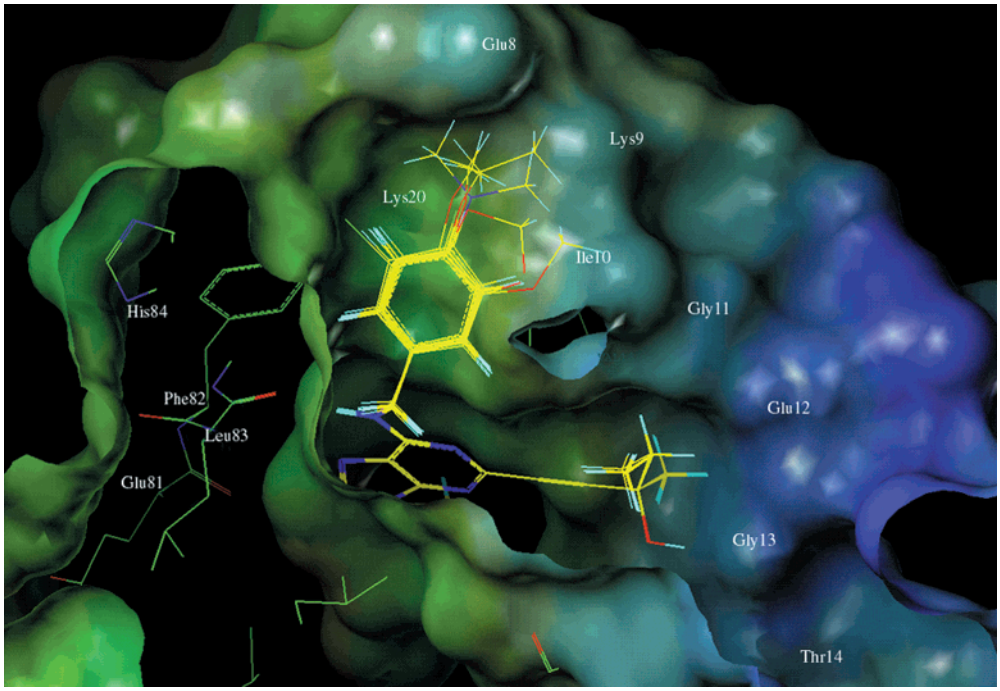

Figure 4. Binding model of **4b**−**h** in the CDK2 active site. See legend of Figure 3 for colors.

interaction, as there is very little difference in the disposition of these entities in the two crystal structures.

In the olomoucine−CDK2 structure, interaction of the phenyl ring of the 6-benzylamine substituent with the δ-amino group of Lys89 was also considered important.[18] In our structure of OL567 complexed to CDK2, the Lys89 side chain adopts a different orientation, and this interaction was consequently not present in our model. Overall, it is probable that any weakening of hydrophobic interactions of the aryl ring in **4e** resulting from *p*-chloro substitution can be more than compensated for by formation of a hydrogen bond between the chlorine atom and the protonated side chain carboxylic acid function of Glu8. However, as this acidic residue is present in its carboxylate form in the model enzyme, this interaction could not be observed in the docking experiment.

Returning to the *m*,*p*-dichloro analogue **4d**, relative to **4a** and **4e**, a slight rotation of the phenyl ring is induced to relieve steric interactions involving the *m*-chloro atom and Phe82. This phenomenon, combined with the accentuated decrease in electron density in the aromatic ring, may well lead to a weakening of the CH−π interaction with Ile10 located directly below it and thereby to the observed sharp drop in activity.

The increased activity of the *p*-methoxy-substituted compound **4b** (OL567) and the corresponding *p*-OEt analogue **4c** compared to the disubstituted compound **4g** is most probably a consequence of their reduced steric volume. However, as they remain essentially equipotent with the parent compound **4a**, it is clear that there is no net advantage in effecting *p*-O-alkoxy substitution of the aromatic ring. One can argue that for these molecules there would be an enhanced positive interaction with Ile10, but it is apparent, even from the X-ray data for OL567, that a nonnegligible steric interaction exists between these groups and Glu8.

Taking into consideration this subtle balance between the stabilizing hydrophobic π type interaction with Ile10 and the destabilizing steric interaction evoked when bulky groups are present on the phenyl ring, it is pertinent to note the good level of activity observed for the *N*-dimethyl compound **4h**. Due to the planar character of the nitrogen atom in this analogue, transfer of electron density to the ring may strengthen the Phe−Ile10 contact. In addition, the orientation of the dimethyl substituent relative to Glu8 was found to be different to that of **4f** and **4g** and may also be at the origin of the increased inhibition of CDK1−cyclin B by this molecule.

For the series of 6-anilino analogues **5** the aromatic ring has a different orientation such that it is deeper in the cleft and rotated by about 45° with respect to the planar nitrogen (Figure 5). As a result, the Ile10 side chain moved slightly so as to preserve CH−π interactions.

The presence of a substituent on the aromatic ring appears to be important for these 6-anilino analogues, as compounds **5b**−**e** are all more active than **5a**. In particular, a hydrogen bond between the alkoxide oxygen and the side chain amino group of Lys89 (NH−O = 2.70 Å) is observed for the *p*-OMe-substituted compound **5b** and the *p*-OEt-substituted compound **5c**. Not neglecting that the para position in compounds **5** is surface exposed, advantage can be taken of the contact with Lys89 in the development of new analogues of our 2-alkynylated purines.

The meta′ position is in close contact with the inner surface of the binding pocket (Asp86 and Lys89). However, the presence of two chlorine atoms (**5d**) decreased the activity, due to unfavorable interactions between the *p*-chlorine atom and the backbone carbonyl group of His84. Furthermore, due to the orientation of the phenyl ring toward the more hydrophilic outside of the cleft, unfavorable interactions are created by the presence of two chlorine atoms which increase its hydrophobic character.

In line with the activities observed for the Novartis compound[10] as well as purvalanols A and B,[12] *m*-chloro

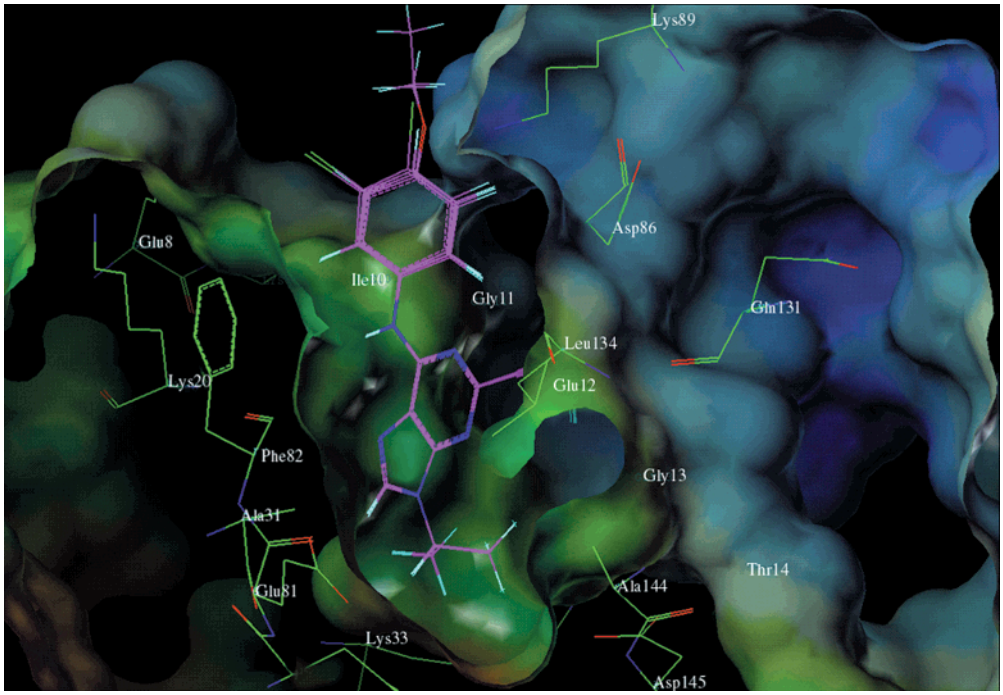

Figure 5. Binding model of **5b**−**e** in the CDK2 active site. See legend of Figure 3 for colors.

substitution as in **5e** resulted in a very pronounced increase in activity. From the X-ray structure of purvalanol B−CDK2[11] it was deduced that an H-bond between the 3-Cl and Asp86 is important. However, the meta′ orientation was privileged only to the extent of 2:1.[11] In our model, this tendency is inversed, the conformer with the chloro substituent in the meta orientation being more stable by 1.5 kcal. This meta′/meta inversion is a consequence of the protonation state of the amine/carboxylic acid functionalities in the protein model (CO_2^-, NH_3^+; pH 7) and also the result of a different orientation in the Asp86 side chain in our crystal structure compared to the purvalanol B−CDK2 X-ray crystal structure. Conversely, in its protonated state, the carboxylate of Asp86 should be engaged in a weak hydrogen bond with the *m′*-chlorine. In any event, irrespective of the preferred conformation for the 3-chloro substituent, it is clear that there is sufficient room available in the enzyme for simultaneous substitution of meta and meta′ positions. This suggestion from our model is currently being explored, but already Schultz et al. have recently shown that a meta,meta′-disubstituted analogue of purvalanol (*m*-Cl,*m′*-NH_2, **97**) is equipotent (IC_{50} = 33 nM) with purvalanol A (IC_{50} = 35 nM) itself.[12]

No ortho/ortho′-substituted products were evaluated, but the presence of functionality at these positions would again generate very unfavorable steric interactions with both neighboring residues (ortho with Phe82, ortho′ with Asp86 and Lys89) and the adenine ring.

Conclusion

The X-ray crystal structure of the OL567−CDK2 complex gives a direct view of the positioning of OL567 in the ATP binding site of the kinase and thereby provided the opportunity to analyze the interactions that exist between this inhibitor and the protein. This information further provided a valid starting point for a broader molecular modeling study of the binding of the entire series of analogues **4** and **5** in the ATP pocket of CDK2. Given the high level of sequence homology between CDK1 and CDK2 (Table 2), the derived models were used to interpret the results obtained in our CDK1−cyclin B activity assay.

For the further design of new purine-based CDK1/2 inhibitors, the results suggest that small polar substituents can be introduced at the para position of series **4** and the meta or para position of **5**, but that substitution at the ortho position of the aromatic ring in both series should be avoided. This study also indicates that only small substituents will be tolerated at the phenyl meta and even more at the meta′ positions in the anilino series. However, any meta′ substituent able to make strong favorable electrostatic or hydrogen-bonding interactions with Lys89 would be expected to result in increased activity.

From the modeling study, it would also appear that key interactions may be conserved if the aromatic ring in compounds **4** and **5** is replaced by certain heterocyclic systems.

Confirmation that the acetylene moiety in **4** and **5** effectively occupies the ribose binding pocket of ATP was another important aspect of our structural study. Indeed, it is remarkable that the 2-nitrogen which is characteristic of all other purine-based CKIs can be replaced by a sp-hybridized carbon atom. Pertinent in this repect is the observation that partial or total reduction of the acetylenic moiety leads to compounds with greatly attenuated activities (IC_{50} > 1000 nM).[16] Finally, comparison of the activities of purvalanol A and the Novartis compounds with **5e**, as well as OL567 with the corresponding purvalanol derivative with a *p*-OMe group (compound **75** in ref 12; IC_{50} = 230 nM), shows that our acetylene-based molecules are of comparable activity. This observation offers a number of interesting possibilities for the construction of new molecules modified both at the C-6 position and in the propargyl side chain, which bind strongly to CDK1/2. In particular, this

Table 2. Selected Amino Acids in CDK2 That Interact with Inhibitors* and Corresponding Amino Acids§ in CDK1, CDK4, CDK5, and CDK6

CDK2[a]	CDK1[b]	CDK5[c]	CDK4[a]	CDK6[a]
Glu8	Glu	Glu	**Ala**[d]	**Ala**
Ileu10	Ileu	Ileu	Ileu	Ileu
Glu12	Glu	Glu	**Val**	Glu
Gly13	Gly	Gly	Gly	Gly
Thr14	Thr	Thr	**Ala**	**Ala**
Val18	Val	Val	Val	Val
Ala31	Ala	Ala	Ala	Ala
Lys33	Lys	Lys	Lys	Lys
Phe80	Phe	Phe	Phe	Phe
Glu81	Glu	Glu	Glu	Glu
Phe82	Phe	Phe	**His**	**His**
Leu83	Leu	**Cys**	**Val**	**Val**
His84	**Ser**	**Asp**	**Asp**	**Asp**
Gln85	**Met**	Gln	Gln	Gln
Asp86	Asp	Asp	Asp	Asp
Lys89	Lys	Lys	**Thr**	**Thr**
Gln131	Gln	Gln	**Glu**	Gln
Asn132	Asn	Asn	Asn	Asn
Leu134	Leu	Leu	Leu	Leu
Ala144	Ala	Ala	Ala	Ala
Asp145	Asp	Asp	Asp	Asp

*Olomoucine, roscovitine, and OL567. § According to sequence comparisons of human CDKs, as described; see [a] Brotherton[39] and Lawrie,[20] [b] De Bondt,[17] [c] Meyerson.[40] [d] Amino acid residues in bold type indicate sequence differences with respect to CDK2.

information will be valuable to current efforts to establish the molecular basis for the observed selectivity of our 2-acetylenylpurine analogues for inhibition of CDK1−cyclin B. Indeed, these molecules, as well as roscovitine and other trisubstituted purines, show a pronounced specificity for inhibition of CDK1, CDK2, and CDK5,[8,9,11] displaying essentially no capacity to inhibit CDK4− and CDK6−cyclin complexes. Indeed, although the crystal structure of CDK6 bound to $p19^{INK4d}$ has been published recently,[39] crystal structures of CDK4 or CDK6, either alone or bound to a cyclin, will be very helpful to understand the absence of activity of most synthetic inhibitors of CDK1 and CDK2 toward CDK4 and CDK6. However, this inactivity is probably the consequence of critical sequence differences between CDK4 and CDK6 (see Table 2) and CDK1, CDK2, and CDK5. These latter three enzymes show a high degree of homology particularly in the catalytic site (Table 2). Several CDK2 residues which in this study have been shown to interact with OL567 and other members of series **4** and **5** by sequence alignment are different in CDK4 and CDK6.

In conclusion, the present study has contributed to a better understanding of the SAR of the new class of acetylenic purine CKIs. This insight will serve as a guide in the design of more potent and selective CKIs.

Experimental Section

Chemistry. The melting points were taken on a Kofler hot stage apparatus and are uncorrected. Elemental analyses were performed by the "Service de Microanalyse", CNRS, ICSN, 91198 Gif sur Yvette, France. Proton nuclear magnetic resonance (^{1}H NMR) spectra were recorded ($CDCl_3$) at 200 MHz on a Bruker AC 200 spectrometer (J values in Hz).

General Procedure for the Preparation of Compounds 2 and 3. A solution of 6-chloro-2-iodo-*9H*-9-isopropylpurine (**1**)[25] in ethanol (40 mL) containing triethylamine (4 equiv) and 1.5 equiv of the appropriate amine was stirred under inert atmosphere (N_2) at 50 °C for 3−4 h. After evaporation of the volatile material in vacuo, workup (CH_2Cl_2 extraction, water washing and $MgSO_4$ drying of the organic phase) was followed by column chromatography which provided pure material after crystallization from heptane.

(2-Iodo-9-isopropyl-*9H*-purin-6-yl)(benzyl)amine (2a) has already been described.[25]

(2-Iodo-9-isopropyl-*9H*-purin-6-yl)(4-methoxybenzyl)-amine (2b). This compound was obtained in 75% yield with mp 188−190 °C. ^{1}H NMR δ: 8.76 (s, 1H), 4.83 (m, 1H), 1.55 (d, 6H, J = 6.7). Anal. ($C_{16}H_{18}N_5O_1I_1$) C, H, N.

(2-Iodo-9-isopropyl-*9H*-purin-6-yl)(4-ethoxybenzyl)-amine (2c). This compound was obtained in 85% yield with mp 174−176 °C. ^{1}H NMR δ: 7.69 (s, 1H, H-8), 7.28 (d, 2H, Phe, J = 8.6), 6.85 (d, 2H, Phe, J = 8.6), 6.31 (br s, 1H, NH), 4.80 (m, 1H, **CH**$(CH_3)_2$), 4.70 (m, 2H, **CH_2**Phe), 4.00 (q, 2H, O**CH_2**CH_3, J = 7), 1.55 (d, 6H, CH(**CH_3**)**$_2$**, J = 6.8), 1.4 (t, 3H, **CH_3**CH_2O, J = 6.9). Anal. ($C_{17}H_{20}N_5O_1I_1$) C, H, N.

(2-Iodo-9-isopropyl-*9H*-purin-6-yl)(3,4-dichlorobenzyl)-amine (2d). A crude solid was obtained in 97% yield with mp 184−186 °C. ^{1}H NMR δ: 7.73 (s, 1H, H-8), 7.47−7.20 (m, 3H, Phe), 6.42 (br s, 1H, NH), 4.89−4.79 (m, 3H, **CH**$(CH_3)_2$, **CH_2**-Phe), 1.56 (d, 6H, CH(**CH_3**)**$_2$**, J = 6.8). Anal. ($C_{15}H_{14}N_5Cl_2I_1$) C, H, N.

(2-Iodo-9-isopropyl-*9H*-purin-6-yl)(4-chlorobenzyl)-amine (2e). This compound was obtained in 87% yield with mp 156−158 °C. ^{1}H NMR δ: 7.68 (s, 1H, H-8), 7,30 (s, 4H, Phe), 6.28 (br s, 1H, NH), 4.81−4.78 (m, 3H, **CH**$(CH_3)_2$, **CH_2**-Phe), 1.55 (d, 6H, CH(**CH_3**)**$_2$**, J = 6.8). Anal. ($C_{15}H_{15}N_5Cl_1I_1$) C, H, N.

(2-Iodo-9-isopropyl-*9H*-purin-6-yl)(3,4-methylenedi-oxybenzyl)amine (2f). This compound was obtained in 93% yield with mp 116−118 °C. ^{1}H NMR δ: 7.85 (s, 1H, H8), 6.89−6.77 (m, 3H, Phe), 5.95 (s, 2H, OCH_2O), 5.05 (m, 1H, **CH**$(CH_3)_2$), 4.77 (m, 2H, **CH_2**Phe), 1.96 (br s, NH,), 1.57 (d, 6H, CH(**CH_3**)**$_2$**). Anal. ($C_{16}H_{16}N_5O_2I_1$) C, H, N.

(2-Iodo-9-isopropyl-*9H*-purin-6-yl)(3,4-dimethoxyben-zyl)amine (2g). This compound was obtained in 97% yield with mp 177−179 °C. ^{1}H NMR δ: 7.91 (br s, 1H, H-8), 7.03−6.81 (m, 3H, Phe), 4.87 (sept, 1H, **CH**$(CH_3)_2$, J = 6.7), 4.72 (br d, 2H, **CH_2**Phe), 3.91 (s, 3H, OCH_3), 3.87 (s, 3H, OCH_3), 2.26 (br s, NH), 1.58 (d, 6H, CH(**CH_3**)**$_2$**, J = 6.7). Anal. ($C_{17}H_{20}N_5O_2I_1$) C, H, N.

(2-Iodo-9-isopropyl-*9H*-purin-6-yl)(4-dimethylaminoben-zyl)amine (2h). This compound was obtained in 72% yield with mp 202−204 °C. ^{1}H NMR δ: 7.61 (s, 1H, H-8), 7.26 (d, 2H, Phe, J = 8.5), 6.76 (d, 2H, Phe, J = 7.9), 6.31 (br s, 1H, NH), 4.80 (sept, 1H, **CH**$(CH_3)_2$, J = 6.9), 4.65 (m, 2H, **CH_2**-Phe), 2.95 (s, 6H, $N(CH_3)_2$), 1.54 (d, 6H, CH(**CH_3**)**$_2$**, J = 6.8). Anal. ($C_{17}H_{21}N_6I_1$) C, H, N.

(2-Iodo-9-isopropyl-*9H*-purin-6-yl)(phenyl)amine (3a). This compound was obtained in 90% yield with mp 124−127 °C. ^{1}H NMR δ: 7.80−7.73 (m, 2H, Phe), 7.61 (s, 1H, H-8), 7.43−7.35 (m, 2H, Phe), 7.15−7.10 (m, 1H, Phe), 4.86 (sept, 1H, **CH**$(CH_3)_2$)), 1.60 (d, 6H, CH(**CH_3**)**$_2$**, J = 6.7). Anal. ($C_{14}H_{14}N_5I_1$·0.3 heptane) C, H, N.

(2-Iodo-9-isopropyl-*9H*-purin-6-yl)(4-methoxyphenyl)-amine (3b). This compound was obtained in 95% yield with mp 147−149 °C. ^{1}H NMR δ: 7.86 (s, 1H, H-8), 7.65 (d, 2H, Phe, J = 8.6), 6.92 (d, 2H, Phe, J = 8.7), 4.87 (sept, 1H, **CH**$(CH_3)_2$, J = 6.7), 3.82 (s, 3H, OCH_3), 1.60 (d, 6H, CH(**CH_3**)**$_2$**, J = 6.7). Anal. ($C_{15}H_{16}N_5O_1I_1$) C,H, N.

(2-Iodo-9-isopropyl-*9H*-purin-6-yl)(4-ethoxyphenyl)-amine (3c). This compound was obtained in 98% yield with mp 136−138 °C. ^{1}H NMR δ: 7.89 (br s, 1H, NH), 7.84 (s, 1H, H-8), 7.64 (d, 2H, Phe, J = 9), 6.92 (d, 2H, Phe, J = 9), 4.87 (sept, 1H, **CH**$(CH_3)_2$, J = 6.7), 4.05 (q, 2H, O**CH_2**CH_3, J = 7), 1.60 (d, 6H, CH(**CH_3**)**$_2$**, J = 6.7), 1.42 (t, 3H, **CH_3**CH_2O, J = 6.9). Anal. ($C_{16}H_{18}N_5O_1I_1$) C, H, N.

(2-Iodo-9-isopropyl-*9H*-purin-6-yl)(3,4-dichlorophenyl)-amine (3d). This compound was obtained in 36% yield with mp 184−186 °C. ^{1}H NMR δ: 8.2 (br s, 1H, NH), 8.02 (m, 1H, Phe), 7.94 (s, 1H, H-8), 7.67−7.62 (m, 1H, Phe), 7.45−7.40 (m, 1H, Phe), 4.89 (m, 1H, **CH**$(CH_3)_2$), 1.62 (d, 6H, CH(**CH_3**)**$_2$**, J = 6.7). Anal. ($C_{14}H_{12}N_5Cl_2I_1$) C, H, N.

(2-Iodo-9-isopropyl-*9H*-purin-6-yl)(3-chlorophenyl)-amine (3e). This compound was obtained in 73% yield with

mp 108−112 °C. ^{1}H NMR δ: 8.01 (s, 1H, H-8), 7.87 (m, 2H, Phe, NH), 7.66−7.63 (m, 1H, Phe), 7.34−7.30 (m, 1H, Phe), 7.11−7.07 (m, 1H, Phe), 4.92−4.88 (m, 1H, **CH**$(CH_3)_2$)), 1.60 (d, 6H, CH(**CH$_3$)$_2$**, J = 6.8). Anal. ($C_{14}H_{13}N_5Cl_1I_1$) C, H, N.

General Procedure for the Preparation of Compounds 4 and 5. A solution of 6-aryl-2-iodo-*9H*-9-isopropylpurine **2** or **3** (1 mmol), CuI (0.05 mmol), bis(triphenylphosphine)palladium dichloride (0.01 mmol), *n*-butylamine (1.5 mmol), and (*R*,*S*)-3-methyl-1-pentyn-3-ol (1.5 equiv) in degassed DMF (25 mL) was stirred under argon atmosphere at 80 °C until disappearance of the iodopurine, as judged by TLC in CH_2Cl_2−EtOH: 95−5. After evaporation of the solvent the residue was dissolved in CH_2Cl_2 and H_2S gas was bubbled into the solution for 2 min.The suspension was evaporated to dryness and subjected to silica gel column chromatography. When necessary, analytical samples were obtained after recrystallization from heptane. Melting points refer to analytical samples.

(3*R*,*S*)-1-[6-Benzylamino-9-isopropyl-*9H*-purin-2-yl]-3-methylpent-1-yn-3-ol (4a) has already been described.[16]

(3*R*,*S*)-1-[9-Isopropyl-6-(4-methoxybenzylamino)-*9H*-purin-2-yl]-3-methylpent-1-yn-3-ol (4b). This compound was obtained in 97% yield with mp 133−136 °C. ^{1}H NMR δ: 7.32 (d, 2H, Phe, J = 8.4), 6.86 (d, 2H, Phe), 3.80 (s, 3H, OCH_3), other protons are identical to **5d**. Anal. ($C_{22}H_{27}N_5O_2$) C, H, N.

(3*R*,*S*)-1-[6-(4-Ethoxybenzylamino)-9-isopropyl-*9H*-purin-2-yl]-3-methylpent-1-yn-3-ol (4c). This compound was obtained in 64% yield with mp 110−114 °C. ^{1}H NMR δ: 7.30 (d, 2H, Phe, J = 8.4), 6.85 (d, 2H, Phe, J = 8.3), 4.01 (q, 2H, O**CH$_2$**CH_3, J = 6.9), 1.40 (t, 3H, OCH_2**CH$_3$**), other protons are identical to **4d**. Anal. ($C_{23}H_{29}N_5O_2$) C, H, N.

(3*R*,*S*)-1-[6-(3,4-Dichlorobenzylamino)-9-isopropyl-*9H*-purin-2-yl]-3-methylpent-1-yn-3-ol (4d). This compound was obtained in 72% yield with mp 114−117 °C. ^{1}H NMR δ: 7.89 (br s, 1H, H-8), 7.50 (m, 1H, Phe), 7.38 (m, 1H, Phe), 7.22 (m, 1H, Phe), 6.6 (br s, 1H, NH), 4.91 (m, 3H, **CH**$(CH_3)_2$, **CH$_2$**-Ph), 1.83 (q, 2H, **CH$_2$**CH_3, J = 7.3), 1.61 (s, 3H, CH_3), 1.58 (d, 6H, CH(**CH$_3$)$_2$**, J = 6.8), 1.14 (t, 3H, CH_2**CH$_3$**, J = 7.4). Anal. ($C_{21}H_{23}N_5O_1Cl_2$) C, H, N.

(3*R*,*S*)-1-[6-(4-Chlorobenzylamino)-9-isopropyl-*9H*-purin-2-yl]-3-methylpent-1-yn-3-ol (4e). This compound was obtained in 54% yield with mp 138−142 °C. ^{1}H NMR δ: 7.86 (br s, 1H, H-8), 7.50 (m, 1H, Phe), 7.29−7.24 (m, 4H, Phe), 6.4 (br s, 1H, NH), 4.89 (m, 3H, **CH**$(CH_3)_2$, **CH$_2$**Ph), 1.82 (q, 2H, **CH$_2$**CH_3, J = 7.3), 1.58 (d, 6H, CH(**CH$_3$)$_2$**, J = 6.8), 1.53 (s, 3H, CH_3), 1.12 (t, 3H, CH_2**CH$_3$**, J = 7.3). Anal. ($C_{21}H_{24}N_5O_1Cl_1$) C, H, N.

(3*R*,*S*)-1-[9-Isopropyl-6-(3,4-methylenedioxybenzylamino)-*9H*-purin-2-yl]-3-methylpent-1-yn-3-ol (4f). This compound was obtained in 68% yield with mp 133−135 °C. ^{1}H NMR δ: 7.85 (br s, 1H, H-8), 6.93−6.70 (m, 3H, Phe), 5.93 (s, 2H, OCH_2O), 5.00−4.66 (m, 3H, **CH**$(CH_3)_2$, **CH$_2$**Ph); 1.84 (q, 2H, **CH$_2$**CH_3, J = 7.4), 1.60 (s, 3H, CH_3), 1.56 (d, 6H, CH-(**CH$_3$)$_2$**, J = 6.7), 1.13 (t, 3H, CH_2**CH$_3$**, J = 7.4). Anal. ($C_{22}H_{25}N_5O_3$) C, H, N.

(3*R*,*S*)-1-[6-(3,4-Dimethoxybenzylamino)-9-isopropyl-*9H*-purin-2-yl]-3-methylpent-1-yn-3-ol (4g). This compound was obtained in 96% yield with mp 75−77 °C. ^{1}H NMR δ: 7.05−6.70 (m, 3H, Phe), 3.87 (s, 6H, 2x OCH_3), other protons are identical to **4d**. Anal. ($C_{23}H_{29}N_5O_3$) C, H, N.

(3*R*,*S*)-1-[6-(4-Dimethylaminobenzylamino)-9-isopropyl-*9H*-purin-2-yl]-3-methylpent-1-yn-3-ol (4h). This compound was obtained in 88% yield with mp 196−198 °C. ^{1}H NMR δ: 7.27 (d, 2H, Phe, J = 8.0), 6.75 (d, 2H, Phe, J = 8.3), 2.94 (s, 6H, $N(CH_3)_2$), other protons are identical to **4d**. Anal. ($C_{23}H_{30}N_6O_1$) C, H, N.

(3*R*,*S*)-1-[9-Isopropyl-6-(phenylamino)-*9H*-purin-2-yl]-3-methylpent-1-yn-3-ol (5a). This compound was obtained in 95% yield with mp 129−131 °C. ^{1}H NMR δ: 7.98 (br s, 1H, H-8), 7.95−7.85 (m, 2H, Phe), 7.48−7.28 (m, 2H, Phe), 7.20−7.02 (m, 1H, Phe), 4.93 (sept, 1H, **CH**$(CH_3)_2$, J = 6.7), 1.87 (q, 2H, **CH$_2$**CH_3, J = 7.4), 1.63 (s, 3H, CH_3); 1.58 (d, 6H, CH-(**CH$_3$)$_2$**, J = 6.7). 1.17 (t, 3H, CH_2**CH$_3$**, J = 7.4). Anal. ($C_{20}H_{23}N_5O_1$·1/4H_2O) C, H, N.

(3*R*,*S*)-1-[9-Isopropyl-6-(4-methoxyphenylamino)-*9H*-purin-2-yl]-3-methylpent-1-yn-3-ol (5b). This compound was obtained in 95% yield with mp 169−171 °C. ^{1}H NMR δ: 8.01 (br s, 1H, H-8), 7.69 (d, 2H, Phe, J = 8.7), 6.92 (d, 2H, Phe, J = 8.8), 3.82 (s, 3H, OCH_3), other protons are identical to **5a**. Anal. ($C_{21}H_{25}N_5O_2$) C, H, N.

(3*R*,*S*)-1-[6-(4-Ethoxyphenylamino)-9-isopropyl-*9H*-purin-2-yl]-3-methylpent-1-yn-3-ol (5c). This compound was obtained in 48% yield with mp 146−148 °C. ^{1}H NMR δ: 7.98 (br s, 1H, H-8), 7.68 (d, 2H, Phe, J = 8.8), 6.90 (d, 2H, Phe, J = 8.8), 4.03 (q, 2H, O**CH$_2$**CH_3, J = 7.0), 1.42 (t, 3H, OCH_2**CH$_3$**, J = 7.0), other protons are identical to **5a**. Anal. ($C_{22}H_{27}N_5O_2$) C, H, N.

(3*R*,*S*)-1-[6-(3,4-Dichlorophenylamino)-9-isopropyl-*9H*-purin-2-yl]-3-methylpent-1-yn-3-ol (5d). This compound was obtained in 66% yield with mp 175−178 °C. ^{1}H NMR δ: 8.23 (s, 1H, H-8), 7.94 (br s, 1H, NH), 7.61−7.57 (m, 1H, Phe), 7.41−7.37 (m, 1H, Phe), 4.95 (sept, 1H, **CH**$(CH_3)_2$, J = 6.7), 1.87 (q, 2H, **CH$_2$**CH_3, J = 7.3), 1.64 (s, 3H, CH_3), 1.61 (d, 6H, CH(**CH$_3$)$_2$**, J = 6.8). 1.19 (t, 3H, CH_2**CH$_3$**, J = 7.3). Anal. ($C_{20}H_{21}N_5O_1Cl_2$) C, H, N.

(3*R*,*S*)-1-[6-(3-Chlorophenylamino)-9-isopropyl-*9H*-purin-2-yl]-3-methylpent-1-yn-3-ol (5e). This compound was obtained in 68% yield with mp 152−155 °C. ^{1}H NMR δ: 8.25−8.05 (br m, 3H, H-8, Phe, NH), 7.63−7.58 (m, 1H, Phe), 7.31−7.26 (m, 1H, Phe), 7.08−7.05 (m, 1H, Phe), 4.95 (sept, 1H, **CH**$(CH_3)_2$, J = 6.7), 1.87 (q, 2H, **CH$_2$**CH_3, J = 7.4), 1.64 (s, 3H, CH_3), 1.61 (d, 6H, CH(**CH$_3$)$_2$**, J = 6.8), 1.19 (t, 3H, CH_2**CH$_3$**, J = 6.8). Anal. ($C_{20}H_{22}N_5O_1Cl_1$) C, H, N.

Expression, Purification, and Crystallization of Human CDK2. Human CDK2 was expressed in Sf9 insect cells using a recombinant baculovirus encoding CDK2 and purified following the published method.[33] Monomeric unphosphorylated CDK2 crystals were grown as described.[20]

Data Collection and Processing. The CDK2−OL567 dataset was collected from a crystal soaked for 60 h in 1 mM OL567 in 1× mother liquor solution (50 mM NH_4Ac, 10% PEG 4K, 0.1 M HEPES, pH 7.4) plus 20% DMSO. Data were collected on beamline X-RAY DIFFRACTION at Elettra, Trieste, operating at a wavelength of 0.90 Å using a Mar 345 detector and oscillations of 1.5°/frame. The crystal was transferred briefly to cryoprotectant (1× mother liquor plus 25% glycerol) before mounting and freezing to 100 K in a nylon loop. Images were integrated with the DENZO[41] package and subsequently scaled and merged using SCALEPACK.

Structure Solution and Refinement. The starting model for the structure solution and refinement of the CDK2−OL567 structure was that of CDK2 in complex with a small molecule inhibitor refined at 1.4 Å resolution.[42] This model includes protein residues 1−35 and 44−296. Residues 36−43 prior to the C-helix are disordered and have not been built in any reported monomeric CDK2 structure. Residues 297 and 298 in this structure are also disordered. Refinement was begun by carrying out rigid body refinement of the CDK2 structure. As the resolution of the data included was increased from 2.5 to 1.9 Å an increasing number of rigid bodies was used, so that initially the whole molecule was treated as two rigid bodies, and finally 10 amino acid segments were allowed to refine independently. The OL567 structure was built in Sybyl[43] and at this point the $(F_o - F_c)_{calc}$ maps included readily interpretable electron density for the bound inhibitor. Refinement of the model was then pursued with alternating cycles of interactive model building[44] and maximum likelihood refinement using the program REFMAC.[45] Toward the end of refinement, water molecules were added using ARP.[46] Statistics relating to the quality of the dataset and of the refined model are presented in Table 3.

CDK1−Cyclin B Assay. CDK1−cyclin B was extracted in homogenization buffer (60 mM β-glycerophosphate, 15 mM *p*-nitrophenylphosphate, 25 mM MOPS (pH 7.2), 15 mM EGTA, 15 mM $MgCl_2$, 1 mM dithiothreitol, 1 mM sodium vanadate, 1 mM NaF, 1 mM phenylphosphate, 10 μg leupeptin/mL, 10 μg aprotinin/mL, 10 μg soybean trypsin inhibitor/mL and 100 μM benzamidine) from M phase starfish (*Marthast-*

Table 3. Statistics of the Datasets Used and of the Refined Structure

data collected (space group *P*212121)	CDK2−OL567
cell dimensions (Å)	53.14, 71.47, 71.91
maximal resolution (Å)	1.80
observations	67163
unique reflections, completeness (%)	25001, 95.8
R_{merge}[a]	0.072
mean $I/\sigma(I)$	8.4
protein atoms	2338
residues	1−35, 44−298
other atoms	298 water 29 OL567
resolution range (Å)	20.00−1.85
R_{conv}[b]	0.19
R_{free}[c]	0.25
mean protein temperature factors (Å)[b]	24.0
mean ligand temperature factors (Å)[b]	34.2

[a] $R_{merge} = \sum_h\sum_j|I_{h,j} - \overline{I_h}|/\sum_h\sum_j|I_{h,j}|$, where $I_{h,j}$ is the jth observation of reflection h. [b] $R_{conv} = \sum_h||F_{oh}| - |F_{ch}||/\sum_h|F_{oh}|$, where F_{oh} and F_{ch} are the observed and calculated structure factor amplitudes, respectively, for reflection h. [c] R_{free} is equivalent to R_{conv} for a 5% subset of reflections not used in the refinement.

erias glacialis) oocytes and purified by affinity chromatography on p9CKShs1-Sepharose beads, from which it was eluted by free p9CKShs1 as previously described. The kinase activity was assayed in buffer C (homogenization buffer but 5 mM EGTA, no NaF and no protease inhibitors) with 1 mg histone H1 (Sigma type III-S)/mL, in the presence of 15 μmol [γ-^{32}P]-ATP (3000 Ci/mmol; 1 mCi/mL) in a final volume of 30 μL and at 30 °C. After a 10-min incubation at 30 °C, 25-μL aliquots of supernatant were spotted onto 2.5 × 3 cm pieces of Whatman P81 phosphocellulose paper, and 20 s later, the filters were washed five times (for at least 5 min each time) in a solution of 10 mL of phosphoric acid/L of water. The wet filters were transferred into 6-mL plastic scintillation vials, 5 mL of ACS (Amersham) scintillation fluid was added and the radioactivity was measured in a Packard counter. Blank values were subtracted from the data and activities calculated as pmoles of phosphate incorporated in protein acceptor for a 10-min incubation. Controls were performed with appropriate dilutions of Me_2SO. IC_{50} values were calculated from dose−response curves.

Acknowledgment. We are indebted to the Association pour la Recherche sur le Cancer (ARC, Subvention No. 9814 to M.L. and ARC 9314 to L.M.) as well as the Conseil Régional de Bretagne (to L.M.) for financial support. We thank the beamline scientists at SRS, Daresbury, ESRF, Grenoble, and Elettra, Trieste, for their assistance during data collection. At the LMB, Oxford, we thank A. Lawrie for preparation of CDK2, E. Garman for assistance during data collection, I. Taylor, and S. Lee. This work was supported by the MRC, BBSRC, and The Royal Society.

Supporting Information Available: Analytical data. This material is available free of charge via the Internet at http://pubs.acs.org.

References

(1) Keyomarsi, K.; Grana, X. In *Progress in Cell Cycle Research*; Meijer, L. G., Philippe, M., Eds.; Plenum Press: New York, 1997; pp 171−191.
(2) Morgan, D. O. Principles of CDK regulation. *Nature* **1995**, *374*, 131−134.
(3) Ball, K. L.; Lain, S.; Fahraeus, R.; Smythe, C.; Lane, D. P. Cell-cycle arrest and inhibition of CDK4 activity by small peptides based on the carboxy-terminal domain of p21^{WAF1}. *Curr. Biol.* **1996**, *7*, 71−80.
(4) Kiyokawa, H.; Kineman, R. D.; Manova-Todorova, K. O.; Soares, V. C.; Hoffman, E. S.; Ono, M.; Khanam, D.; Hayday, A. C.; Frohman, L. A.; Koff, A. Enhanced growth of mice lacking the cyclin-dependent kinase inhibitor function of p27^{Kip1}. *Cell* **1996**, *85*, 721−732.
(5) Hui, A. M.; Sun, L.; Kanai, Y.; Sakamoto, M.; Hirohashi, S. Reduced p27(Kip1) expression in hepatocellular carcinomas. *Cancer Lett.* **1998**, *132*, 67−73.
(6) Hanks, S. K.; Quinn, A.-M.; Hunter, T. The protein kinase family: Conserved features and deduced phylogeny of the catalytic domains. *Science* **1988**, *241*, 42−52.
(7) Taylor, S. S.; Radzio-Andzelm, E. Three protein kinase structures define a common motif. *Structure* **1994**, *2*, 345−355.
(8) Veseley, J.; Havlicek, L.; Strnad, M.; Blow, J. J.; Donella-Deana, A.; Pinna, L.; Letham, D. S.; Kato, J.-Y.; Detivaud, L.; Leclerc, S.; Meijer, L. Inhibition of cyclin-dependent kinases by purine analogues. *Eur. J. Biochem.* **1994**, *224*, 771−786.
(9) Meijer, L.; Borgne, A.; Mulner, O.; Chong, J. P. J.; Blow, J. J.; Inagaki, N.; Inagaki, M.; Delcros, J. G.; Moulinoux, J. P. Biochemical and cellular effects of roscovitine, a potent and selective inhibitor of the cyclin-dependent kinases cdc2, cdk2 and cdk5. *Eur. J. Biochem.* **1997**, *243*, 527−536.
(10) Imbach, P.; Capraro, H. G.; Furet, P.; Mett, H.; Meyer, T.; Zimmermann, J. 2,6,9-trisubstituted purines: Optimization towards highly potent and selective CDK1 inhibitors. *Bioorg. Med. Chem. Lett.* **1999**, *9*, 91−96.
(11) Gray, N. S.; Wodicka, L.; Thunnissen, A. M. W. H.; Norman, T. C.; Kwon, S. J.; Espinoza, F. H.; Morgan, D. O.; Barnes, G.; LeClerc, S.; Meijer, L.; Kim, S. H.; Lockhart, D. J.; Schultz, P. G. Exploiting chemical libraries, structure, and genomics in the search for kinase inhibitors. *Science* **1998**, *281*, 533−538.
(12) Chang, Y. T.; Gray, N. S.; Rosania, G. R.; Sutherlin, D. P.; Kwon, S.; Norman, T. C.; Sarohia, R.; Leost, M.; Meijer, L.; Schultz, P. G. Synthesis and application of functionally diverse 2,6,9-trisubstituted purine libraries as CDK inhibitors. *Chem. Biol.* **1999**, *6*, 361−375.
(13) De Azevedo, W. F.; Mueller-Dieckmann, H.-J.; Schulze-Gahmen, U.; Worland, P. J.; Sausville, E.; Kim, S.-H. Structural basis for specificity and potency of a flavonoid inhibitor of human CDK2, a cell cycle kinase. *Proc. Natl. Acad. Sci. U.S.A.* **1996**, *93*, 2735−2740.
(14) Hoessel, R.; Leclerc, S.; Endicott, J.; Noble, M.; Lawrie, A.; Tunnah, P.; Leost, M.; Damiens, E.; Marie, D.; Marko, D.; Niederberger, E.; Tang, W.; Eisenbrand, G.; Meijer, L. Indirubin, the active constituent of a chinese antileukeamia medicine, inhibits cyclin-dependent kinases. *Nature Cell Biol.* **1999**, *1*, 60−67.
(15) Schultz, C.; Link, A.; Leost, M.; Zaharevitz, D. W.; Gussio, R.; Sausville, E. A.; Meijer, L.; Kunick, C. Paullones, a series of cyclin-dependent kinase inhibitors: synthesis, evaluation of CDK1/cyclin B inhibition, and in vitro antitumor activity. *J. Med. Chem.* **1999**, *42*, 2909−2919.
(16) Legraverend, M.; Ludwig, O.; Bisagni, E.; Leclerc, S.; Meijer, L. Synthesis of C2 alkynylated purines, a new family of potent inhibitors of cyclin-dependent kinases. *Bioorg. Med. Chem. Lett.* **1998**, *8*, 793−798.
(17) De Bondt, H. L.; Rosenblatt, J.; Jancarik, J.; Jones, H. D.; Morgan, D. O.; Kim, S.-H. Crystal structure of cyclin-dependent kinase 2. *Nature* **1993**, *363*, 595−602.
(18) Schulze-Gahmen, U.; Brandsen, J.; Jones, H. D.; Morgan, D. O.; Meijer, L.; Vesely, J.; Kim, S.-H. Multiple modes of ligand recognition: Crystal structures of cyclin-dependent protein kinase 2 in complex with ATP and two inhibitors, olomoucine and isopentenyladenine. *Proteins Struct. Funct. Genet.* **1995**, *22*, 378−391.
(19) De Azevedo, W. F.; Leclerc, S.; Meijer, L.; Havlicek, L.; Strnad, M.; Kim, S. H. Inhibition of cyclin-dependent kinases by purine analogues − Crystal structure of human cdk2 complexed with roscovitine. *Eur. J. Biochem.* **1997**, *243*, 518−526.
(20) Lawrie, A. M.; Noble, M. E. M.; Tunnah, P.; Brown, N. R.; Johnson, L. N.; Endicott, J. A. Protein kinase inhibition by staurosporine revealed in details of the molecular interaction with CDK2. *Nature Struct. Biol.* **1997**, *4*, 796−801.
(21) Jeffrey, P. D.; Russo, A. A.; Polyak, K.; Gibbs, E.; Hurwitz, J.; Massagué, J.; Pavletich, N. P. Mechanism of CDK activation revealed by the structure of a cyclinA-CDK2 complex. *Nature* **1995**, *376*, 313−320.
(22) Russo, A. A.; Jeffrey, P. D.; Patten, A. K.; Massagué, J.; Pavletich, N. P. Crystal structure of the p27^{Kip1} cyclin-dependent-kinase inhibitor bound to the cyclin A-Cdk2 complex. *Nature* **1996**, *382*, 325−331.
(23) Legraverend, M.; Boumchita, H.; Zerial, A.; Huel, C.; Lemaitre, M.; Bisagni, E. Synthesis of new (±)-3,5-dihydroxypentyl nucleoside analogues from 1-amino-5-(benzyloxy)pentan-3-ol and their antiviral evaluation. *J. Med. Chem.* **1990**, *33*, 2476−2480.
(24) Legraverend, M.; Boumchita, H.; Bisagni, E. A new route to 2,5-diamino-4,6-dichloropyrimidine, a key precursor of 9-substituted guanines. *Synthesis* **1990**, 587−590.
(25) Legraverend, M.; Ludwig, O.; Bisagni, E.; Leclerc, S.; Meijer, L.; Giocanti, N.; Sadri, R.; Favaudon, V. Synthesis and in vitro evaluation of novel 2,6,9-trisubstituted purines as cyclin-dependent kinases inhibitors. *Bioorg. Med. Chem.* **1999**, *7*, 1281−1293.

(26) Sonogashira, K.; Tohda, Y.; Hagihara, N. A convenient synthesis of acetylenes: Catalytic substitutions of acetylenic hydrogen with bromoalkenes, iodoarenes, and bromopyridines. *Tetrahedron Lett.* **1975**, 4467−4470.
(27) Sharma, P.; Steinbach, P. J.; Sharma, M.; Amin, N. D.; Barchi, J. J.; Pant, H. C. Identification of substrate binding site of cyclin-dependent kinase 5. *J. Biol. Chem.* **1999**, *274*, 9600−9606.
(28) Chou, K. C.; Watenpaugh, K. D.; Heinrikson, R. L. A model of the complex between cyclin-dependent kinase 5 and the activation domain of neuronal Cdk5 activator. *Biochem. Biophys. Res. Commun.* **1999**, *259*, 420−428.
(29) Norman, T. C.; Gray, N. S.; Hoh, J. T.; Schultz, P. G. A structure-based library approach to kinase inhibitors. *J. Am. Chem. Soc.* **1996**, *118*, 7430−7431.
(30) Schow, S. R.; Mackman, R. L.; Blum, C. L.; Brooks, E.; Horsma, A. G.; Joly, A.; Kerwar, S. S.; Lee, G.; Shiffman, D.; Nelson, M. G.; Wang, X.; Wick, M. M.; Zhang, X.; Lum, R. T. Synthesis and activity of 2,6,9-trisubstituted purines. *Bioorg. Med. Chem. Lett.* **1997**, *7*, 2697−2702.
(31) Zimmerman, J.; Capraro, H. G.; Peterli, P.; Furet, P. Purine derivatives and processes for their preparation. Patent WO 97/16452, 1997.
(32) Meijer, L.; Kim, S. H. Chemical inhibitors of cyclin-dependent kinases. *Methods Enzymol.* **1997**, *283*, 113−128.
(33) Brown, N. R.; Noble, M. E. M.; Lawrie, A. M.; Morris, M. C.; Tunnah, P.; Divita, G.; Johnson, L. N.; Endicott, J. A. Effects of phosphorylation of threonine 160 on cyclin-dependent kinase 2 structure and activity. *J. Biol. Chem.* **1999**, *274*, 8746−8756.
(34) Wallace, A. C.; Laskowski, R. A.; Thornton, J. M. LIGPLOT: a program to generate schematic diagrams of protein−ligand interactions. *Protein Eng.* **1995**, *8*, 127−134.
(35) Rosenblatt, J.; DeBondt, H.; Jancarik, J.; Morgan, D. O.; Kim, S. H. Purification and crystallisation of human cyclin-dependent kinase 2. *J. Mol. Biol.* **1993**, *230*, 1317−1319.
(36) Schulze-Gahmen, U.; De Bondt, H. L.; Kim, S.-H. High-resolution crystal structures of human cyclin-dependent kinase 2 with and without ATP: Bound waters and natural ligand for inhibitor design. *J. Med. Chem.* **1996**, *39*, 4540−4546.
(37) Russo, A.; Jeffrey, P. D.; Pavletich, N. P. Structural basis of cyclin-dependent kinase activation by phosphorylation. *Nature Struct. Biol.* **1996**, *3*, 696−700.
(38) Nishio, M.; Hirota, M. CH/π interaction: Implications in organic chemistry. *Tetrahedron* **1989**, *45*, 7201−7245.
(39) Brotherton, D. H.; Dhanaraj, V.; Wick, S.; Brizuela, L.; Domaille, P. J.; Volyanik, E.; Xu, X.; Parisini, E.; Smith, B. O.; Archer, S. J.; Serrano, M.; Brenner, S. L.; Blundell, T. L.; Laue, E. D. Crystal structure of the complex of the cyclin D dependent kinase Cdk6 bound to the cell-cycle inhibitor p19(INK4d). *Nature* **1998**, *395*, 244−250.
(40) Meyerson, M.; Enders, G. H.; Wu, C.-L.; Su, L.-K.; Gorka, C.; Nelson, C.; Harlow, E.; Tsai, L.-H. A family of human cdc2-related protein kinases. *EMBO J.* **1992**, *11*, 2909−2917.
(41) Otwinowski, Z.; Minor, W. Processing of X-ray diffraction data collected in oscillation mode. *Methods Enzymol.* **1997**, *276*, 307−326.
(42) Calvert, A. H. Unpublished results.
(43) *Sybyl*, 6.3 ed.; SYBYL Molecular Modeling Software, Tripos Associates Ltd.: St. Louis, MO, 1992.
(44) Jones, T. A.; Zou, J. Y.; Cowan, S. W.; Kjeldgaard, M. Improved method for building models in electron density maps and the location of errors in these models. *Acta Crystallogr.* **1991**, *A47*, 110−119.
(45) Murshudov, G. N.; Vagen, A. A.; Dodson, E. J. Refinement of macromolecular structures by the maximum -likelihood method. *Acta Crystallogr.* **1997**, *D53*, 240−255.
(46) Lamzin, V. S.; Wilson, K. S. Automated refinement of protein models. *Acta Crystallogr.* **1993**, *D49*, 129−147.

JM9911130